Electrical modeling of heterojunction silicon solar cells including Indium-Tin-Oxide layers

J. Balent, J. Krc, and M. Topic
University of Ljubljana, Faculty of Electrical Engineering, Trzaska 25, Si-1000 Ljubljana, Slovenia

***Abstract*– In this contribution we performed opto-electrical simulations of heterojunction silicon (HJ Si) solar cell with Indium-Tin-Oxide layers included in simulations as front and rear contacts. Two-dimensional numerical simulations using Sentaurus TCAD software were carried out. We studied the effect of defect state density in p- and n-type hydrogenated amorphous silicon layers on device performance. Rigorous analysis revealed mainly a decrease of *FF* in cases of high levels of defect densities, leading to degradation of conversion efficiency. The increase of defects in p-a-Si proved to be more detrimental than the same increase in n-a-Si, regardless whether the light enters through the p-a-Si or n-a-Si side of the device.**

I. Introduction

Silicon solar cells represent the majority (> 95 %) of the PV market today. The hetero-junction silicon (HJ Si) cell holds the current world record in silicon solar cells with efficiency reaching 26.7 % on a 79 cm^2 wafer [1]. This was achieved by careful optical design (e.g. backside contacting) and especially by optimisation of electrical properties of layers and interfaces in the device (e.g. chemical and electrical surface passivation). Even though the state-of-the-art silicon solar cells are close to reaching the theoretical limit (~ 29 % for Si single junction device), there is still a strong interest to push the device performance towards the limit edge. This can be attained only by an in-depth understanding of remaining optical and electrical loss mechanisms of existing cells. Numerical modelling and simulations are indispensable in the R&D cycle.

In this contribution we present an insight into detailed opto-electrical modelling of HJ Si solar cells, including the Indium-Tin-Oxide (ITO) transparent conductive contacts (TCO) at both sides of the device. In particular, we investigate the role of defect states in p- and n-doped hydrogenated amorphous silicon layers that are used for selective collection of positive (holes) and negative (electrons) charge carriers generated by light in n-type crystalline silicon bulk absorber. More precisely, we study the effect of dangling bond concentrations (N_{db}), see Fig. 1, on current density – voltage (*J-V)* characteristic and on output parameters of the solar cell (J_{SC} – Short-Circuit current density, V_{OC} - Open-Circuit voltage, *FF* – Fill-Factor and *Eff* – Efficiency).

II. Device description and numerical models

The individual layers (and their thickness) of the simulated HJ Si structure are: cathode contact ITO (70 nm), highly defective p-a-Si:H region (1 nm), p-a-Si:H hole collection layer (9 nm), i-a-Si:H passivation layer (5 nm), n-c-Si defect region (2 nm), n-c-Si bulk absorber (150 μm), n-c-Si defective region (2 nm), i-a-Si:H passivation layer (5 nm), n-a-Si:H electron collection layer (9 nm), highly defective n-a-Si:H region (1 nm), ITO (100 nm) anode contact. The p, i and n stand for doping of semiconductors respectively. Light enters the structure through the cathode (p-) side of the device in our case. N_{DB} parameter was varied in p-a-Si:H and n-a-Si:H layers. Some material parameters used in the simulations are presented in TABLE I. Tail and dangling bond defect state distributions are illustrated for the case of p-a-Si:H layer in Figure 1.

Electrical simulations (2-D) were performed with the Sentaurus TCAD [2] software suite. Optical generation was calculated using Sun*Shine* [3] simulator in this case. In electrical simulations we employed the Drift-Diffusion model to calculate the Poisson equation coupled with the continuity equations for holes and electrons. We modelled the Shockley-Read-Hall (SRH) recombination in the n-c-Si as life-time of minority carriers - Holes (10 ms). To properly model amorphous materials, we defined energetic distributions in the energy gap of p, i, n-a-Si by exponential (tail states) and Gaussian (dangling bonds) functions (donor and acceptor like) with parameters taken from [4].

TABLE I
Basic Input Parameters Used in Simulations

Parameter	i-a-Si:H	n-a-Si:H	p-a-Si:H	n-c-Si	ITO
Electron Affinity χ (eV)	3.9	3.9	3.9	4.05	4.7
Band Gap E_g (eV)	1.75	1.80	1.75	1.12	3.7
Doping concentration. N_D/N_A (cm^{-3})	--	5e19 / 0	0 / 5e19	5e15 / 0	1e20 / 0
Effective density of states N_C/N_V (cm^{-3})	2e20 / 2e20	2e20 / 2e20	2e20 / 2e20	2.8e19 / 1.8e19	4.95e18 / 4.95e18
Mobility μ_e/μ_h (cm^{2}V^{-1}s^{-1})	25/5	20/4	25/5	1417 / 470	50/30

978-1-7281-6086-3/20/$31.00 ©2020 IEEE

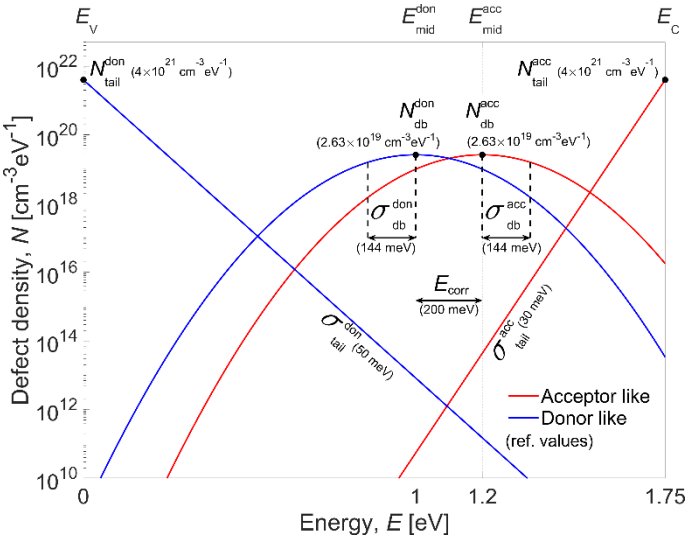

Figure 1 Defect state distribution in p-a-Si with stated reference values. The black symbols show the N_{db} parameters we have varied.

Interface defects at the p, n-a-Si and ITO were defined from the same set of parameters, but their tail and dangling-bond peak defect densities were increased by a factor of 10. Defects at the a-Si/c-Si heterojunctions were modelled only as donor and acceptor-like Gaussian functions with their peaks N_{db}=2.3e19 cm^{-3}eV^{-1} symmetrically placed around the mid-gap energy and 200 meV apart. Auger and radiative recombination were taken into account for all the layers.

Quantum-mechanical effects (thermionic emission and tunnelling) as transport mechanisms were also taken into account [5].

III. Simulation Results and Discussion

Simulation results of variation of N_{db} in p-a-Si:H and n-a-Si:H are presented in the range of 2.63e19 cm^{-3}eV^{-1} (Reference) – 1e20 cm^{-3}eV^{-1}. We varied N_{db} of both Gaussian peaks corresponding to 1.89e19 cm^{-3} – 7.22e19 cm^{-3} total concentration of dangling-bond states. However, they were varied separately for the p-a-Si:H and n-a-Si:H layers. Results are presented in Fig. 2a and 2b. All other defect state parameters were kept constant and are given in Fig. 1.

The increase of N_{db} in p-a-Si brings the cell from its reference efficiency of 25.62 % to 14.87 % at N_{db}=1e20 cm^{-3}eV^{-1} as depicted in Fig.2a. On the other hand, we can notice that the sensitivity of Eff. to increased defects in n-a-Si:H layer is much lower. Simulations revealed that this trend does not depend on the side of illumination (either p-a-Si:H or n-a-Si:H side) or the doping type of the bulk c-Si wafer, but can be attributed to the difference between the valence (2.75 eV) and conduction (0.8 eV) band offsets at the ITO/p-a-Si and n-a-Si/ITO heterojunctions, respectively.

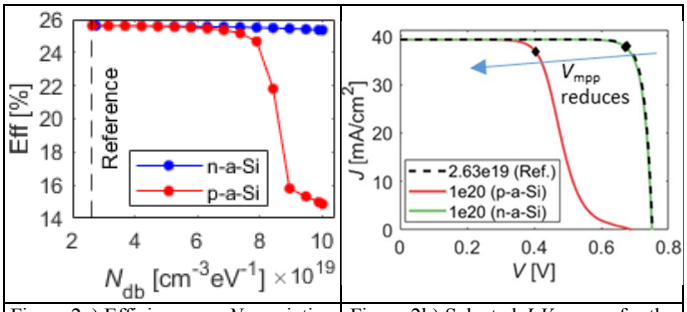

Figure 2a) Efficiency vs. N_{db} variation in p-a-Si and n-a-Si. Changes of N_{db} in p-a-Si lower the efficiency considerably more than that in n-a-Si

Figure 2b) Selected J-V curves for the reference and worst cases in p-a-Si and n-a-Si. Reduction in efficiency can be attributed mainly due to low FF (V_{mpp})

Fig. 2b shows that the drop in efficiency, due to increase of defects in p-a-Si, is on the account of decreased V_{mpp} in the first place and consequently lower FF. By increasing the defects further, also the J_{mpp} starts to drop (not shown here). Detailed inside view in the device, enabled by opto-electrical simulations, revealed that V_{mpp} drop is caused by total charge redistribution (especially by filling the trapped states by carriers) on the p-side of the device. The J_{mpp} drop is small as the recombination level is still much lower than optical generations, despite increased defect states, enhancing recombination.

IV. Conclusions

Variation of N_{db} in p-a-Si affects the cell efficiency much more than variation in n-a-Si. It was observed, that slight increase in N_{db} lowers mostly the FF by reducing the maximum power-point voltage (V_{mpp}). The difference in the effects between variation in p-a-Si and n-a-Si was contributed to the larger barrier for holes (2.75 eV) at the p-a-Si/ITO junction than for electrons at the n-a-Si/ITO (0.8eV) heterojunction, despite tunnelling effects included. Electrical simulations proved to be an efficient tool for detailed investigation of device performance and further optimization.

Acknowledgment

The authors acknowledge the financial support from the Slovenian Research Agency (program P2-0197 and PhD funding for J. Balent).

References

[1] K. Yoshikawa *et al.*, "Silicon heterojunction solar cell with interdigitated back contacts for a photoconversion efficiency over 26%," *Nat. Energy*, vol. 2, no. 5, pp. 1–8, Mar. 2017, doi: 10.1038/nenergy.2017.32.

[2] "TCAD." https://www.synopsys.com/silicon/tcad.html (accessed Apr. 09, 2020).

[3] J. Krc, F. Smole, and M. Topic, "Analysis of light scattering in amorphous Si:H solar cells by a one-dimensional semi-coherent optical model," *Prog. Photovolt. Res. Appl.*, vol. 11, no. 1, pp. 15–26, Jan. 2003, doi: 10.1002/pip.460.

[4] A. Fell *et al.*, "Input Parameters for the Simulation of Silicon Solar Cells in 2014," *IEEE J. Photovolt.*, vol. 5, no. 4, pp. 1250–1263, Jul. 2015, doi: 10.1109/JPHOTOV.2015.2430016.

[5] A. Kanevce and W. K. Metzger, "The role of amorphous silicon and tunneling in heterojunction with intrinsic thin layer (HIT) solar cells," *J. Appl. Phys.*, vol. 105, no. 9, pp. 094507–1, May 2009, doi: 10.1063/1.3106642.